Structural Relaxation of Glass-Forming Polymers Based on an Equation for Configurational Entropy. 2. Structural Relaxation in Polymethacrylates

J. L. Gómez Ribelles,† M. Monleón Pradas,*,† A. Vidaurre Garayo,‡ F. Romero Colomer,‡ J. Más Estellés,‡ and J. M. Meseguer Dueñas‡

Departamento de Termodinámica Aplicada and Departamento de Física Aplicada, Universidad Politécnica de Valencia, P.O. Box 22012, E-46071 Valencia, Spain

Received August 9, 1994; Revised Manuscript Received March 27, 1995®

ABSTRACT: The dependence of the heat capacity on temperature measured in DSC heating scans after different thermal histories in poly(methyl methacrylate), poly(ethyl methacrylate), and poly(butyl methacrylate) is reported. These results are analyzed with the help of a phenomenological model for the evolution of configurational entropy under arbitrary histories. The possibility of obtaining material parameters from the experimental results is discussed. The dependence of the relaxation times in equilibrium conditions on temperature is calculated for the three polymers and compared with the results of the main viscoelastic and dielectric relaxation processes reported in the literature. The width parameter of the Kohlrausch–Williams–Watts relaxation function is also calculated for the three polymers of this series.

1. Introduction

Structural relaxation is the process by which amorphous materials in the glassy state approach a state of thermodynamical equilibrium when held at constant environmental conditions. The process can be detected through the time evolution of thermodynamic properties such as specific volume or enthalpy, as well as through mechanical, dielectric, and other physical properties. The study of the structural relaxation process by means of differential scanning calorimetry (DSC) attracts much attention because of the high reproducibility of the thermal histories of the experiments and the simplicity of the experimental procedure.

In DSC a sample is subjected to a more or less complicated thermal history, which starts at a temperature T_0 higher than the glass transition temperature T_g, with the sample in thermodynamical equilibrium, and involves stages with heating or cooling at constant rates as well as isothermal stages, finishing at a temperature T_1 below T_g. Then, the heat capacity of the sample is measured during a heating scan at a constant rate between T_1 and T_0. The $c_p(T)$ curve thus obtained depends on the thermal history and contains information about the structural relaxation which has taken place previous to the measurement and during the measurement scan itself. In particular, when the thermal history involves an isothermal stage at a temperature close to T_g, the $c_p(T)$ curve shows a characteristic peak that overlaps the glass transition (Figure 1a), but with a lower temperature of the isothermal treatment a peak in the $c_p(T)$ curve at temperatures below T_g (Figure 1b) does show up sometimes. Both types of behavior have been explained in terms of the approach of the enthalpy to equilibrium values during the measuring scan.[1–14] The shape and the temperature of these peaks strongly depend on the time and temperature of the isothermal treatment previous to the measurement.

In ref 15 a modification of the phenomenological model of Scherer and Hodge[16,17] was proposed to follow

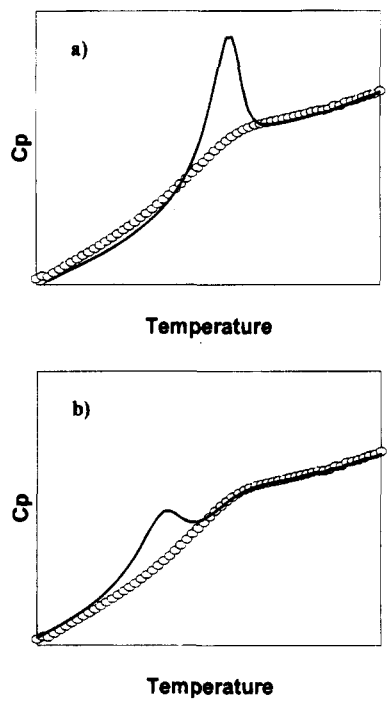

Figure 1. Sketch of the $c_p(T)$ curve measured after an isothermal annealing (a) at a temperature close to T_g and (b) at a lower temperature. The open circles represent the $c_p(T)$ curve measured after cooling the sample at a high rate from a temperature above T_g (see text).

the evolution of the configurational entropy during the structural relaxation process. It is a model with four fitting parameters based on three main assumptions: the use of the reduced time as a variable in the equations of the model, a Kohlrausch–Williams–Watts-like (KWW) relaxation function[18] to account for nonexponentiality, and the use of the Adam–Gibbs[19] theory extended to nonequilibrium conditions to express the dependence of the relaxation times on temperature and structure during the structural relaxation process. The difference with the Scherer–Hodge model lies in the variable chosen to follow the process, which is in our case the configurational entropy, S_c, instead of the fictive temperature, T_f. The evolution of the configu-

† Departamento de Termodinámica Aplicada.
‡ Departamento de Física Aplicada.
® Abstract published in *Advance ACS Abstracts,* July 1, 1995.

0024-9297/95/2228-5878$09.00/0

rational entropy in response to a thermal history that consists of a series of temperature jumps from T_{i-1} to T_i at time instants t_i followed by isothermal stages, is given by

$$S_c(\xi,T) - S_c^{eq}(T) = \sum_{i=1}^{n}\left(\int_{T_i}^{T_{i-1}} \frac{\Delta c_p}{T}\,dT\right)\phi(\xi - \xi_i) \quad (1)$$

where ξ is the reduced time

$$\xi(t) = \int_0^t \frac{dt'}{\tau(t')} \quad (2)$$

and $\xi_i = \xi(t_i)$. The function τ is the extension of the Adam and Gibbs one to nonequilibrium conditions:

$$\tau(T,S_c) = A\exp\left(\frac{B}{TS_c(\xi,T)}\right) \quad (3)$$

and the relaxation function is assumed of the KWW type:

$$\phi(\xi) = \exp(-\xi^\beta) \quad (4)$$

In equilibrium

$$S_c^{eq}(T) = \int_{T_2}^{T}\frac{\Delta c_p}{T'}\,dT' \quad (5)$$

where T_2 is the Gibbs–DiMarzio[20] structural temperature at which the configurational entropy in equilibrium vanishes and $\Delta c_p(T)$ is the configurational heat capacity, usually assumed to be the difference between the experimental values of the heat capacity measured at temperatures above and below the glass transition interval. The model contains four material constants: B, T_2, and A in (3) and (5) and β in (4). All of them are assumed to be independent of the thermal history.

The use of the configurational entropy in the model equations avoids the calculation of the fictive temperature, which needs a previous assumption on the form of the dependence of the configurational heat capacity with temperature. Equations 1–5 are valid for any form of $\Delta c_p(T)$, which makes it easy to study the influence of this form on the overall fit of the model to the experimental results and on the ensuing values of the material parameters.

Many different equations have been proposed for this dependence: from the consideration of Δc_p as independent of temperature to complicated phenomenological equations to describe the heat capacity of the glass of the liquid in a broad temperature interval[22] or the equation deduced from the Gibbs–DiMarzio theory.[20,21] The equations more frequently used in the simulation of the structural relaxation process are

$$\Delta c_p(T) = A_1 + A_2T \quad (6)$$

and

$$\Delta c_p(T) = \frac{T_g\Delta c_p(T_g)}{T} \quad (7)$$

The modeling of the entropy relaxation in polycarbonate[15] has shown that the model reproduces the experimental DSC results with almost the same overall good accuracy when (6 and 7) are used for $\Delta c_p(T)$, or even when Δc_p is considered as a constant. Nevertheless the value of the parameter T_2 found by the search routine is quite dependent on the expression used for $\Delta c_p(T)$. The most significant discrepancy between the model prediction and the experimental $c_p(T)$ curves is the peak occurring in the model $c_p(T)$ curve after an isothermal annealing at a temperature very close to the glass transition temperature T_g: this peak is much higher in the theoretical curve than in the experimental one.

In this work we present experimental DSC results on poly(methyl methacrylate), poly(ethyl methacrylate), and poly(butyl methacrylate) and analyze, with the help of the model predictions, the possibility of determining material parameters for these polymers (independent of the thermal history) and the relationship between the parameters of the model and the molecular structure of these polymers.

2. Experimental Section

Poly(methyl methacrylate) (PMMA, M_w = 350 000) and poly(ethyl methacrylate) (PEMA, M_w = 250 000) from Polysciences Inc., and poly(butyl methacrylate) (PBMA) Elvacite 2044 from DuPont were used in this study. All the samples were molded at about 75 deg above their T_g to sheets approximately 0.3 mm thick, from which the samples for the DSC experiments were cut out. The samples were dried in a vacuum to a constant weight at about 60 deg above T_g.

Calorimetric experiments were carried out in a Perkin-Elmer DSC4 differential scanning calorimeter calibrated with indium and sapphire standards, and data were collected in a TADS 3700 station. For each polymer a single sample of about 10 mg encapsulated in an aluminum pan was used in all the experiments.

All thermal treatments were performed in the calorimeter, and they all started with an annealing at a temperature T_0 for 10 min to ensure that the polymer was in equilibrium and erase the effects of previous thermal histories (T_0 = 150 °C in PMMA, 130 °C in PEMA, and 90 °C in PBMA). Whenever the thermal history included an isothermal annealing at temperature T_a, the cooling rate to attain T_a was q_c = 40 °C/min in the experiments carried out on PMMA and q_c = 20 °C/min in the cases of PEMA and PBMA. These were the highest cooling rates for which the whole cooling process was under control of the temperature programmer (the highest controllable cooling rates depend on the difference between the temperature interval of the experiment and the temperature of the aluminum block of the apparatus that acts as a cold focus. Thus it is higher in the case of PMMA, for which the experimental interval—due to its higher T_g—was higher than in the cases of PEMA and PBMA). After an annealing time t_a the samples were cooled again at the rate q_c until the temperature T_1 selected for the start of the measuring scan (T_1 = 50 °C in PMMA, 30 °C in PEMA, and 10 °C in PBMA) and then heated at 10 °C/min to T_0. The heat flux was measured only on heating, and the $c_p(T)$ curve was calculated from it. We will call hereafter *reference scan* the one carried out on heating at 10 °C/min after a cooling at q_c from T_0 to T_1.

In order to compare the effect of the different thermal treatments on the three polymers, the annealing temperatures were selected to be more or less in the same location in the temperature interval of the glass transition. The glass transition temperature T_g was calculated from the reference scan, as the temperature of the intersection of the enthalpy lines corresponding to equilibrium and to the glassy state, known as the fictive temperature in the glassy state $T_{f'}$. It is defined by (see ref 23)

$$\int_{T_{f'}}^{T^*}(c_{pl}(T) - c_{pg}(T))\,dT = \int_{T_1}^{T^*}(c_p(T) - c_{pg}(T))\,dT \quad (8)$$

where $c_p(T)$ is the specific heat capacity measured during the experimental scan, c_{pl} and c_{pg} are the specific heat capacities of the liquid and the glass, respectively, T^* is a temperature high enough in the liquid state, and T_1 is a temperature low

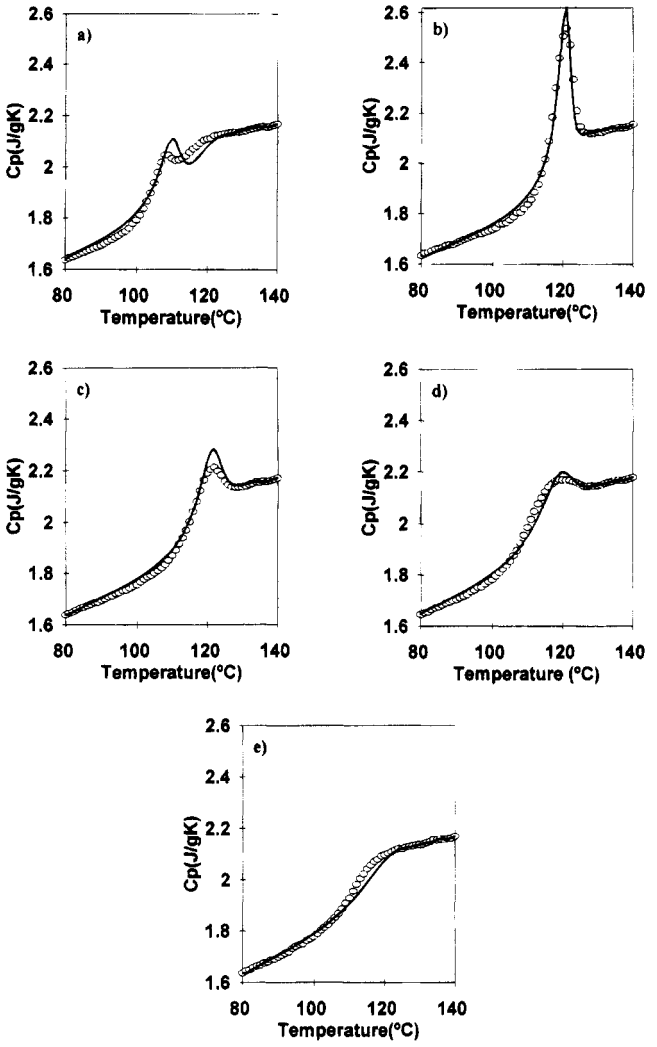

Figure 2. Experimental $c_p(T)$ curves measured on PMMA after thermal histories that include an isothermal annealing at 80 °C for 1037 min (a), 100 °C for 1350 min (b), and 110 °C for 2500 min (c) and after cooling at 1 °C/min (d) and 40 °C/min (e). The solid line represents the prediction of the model with Δc_p according to (6), B = 2000 J/g, and the remaining parameters as shown in Table 2. The circles correspond to the experimental values.

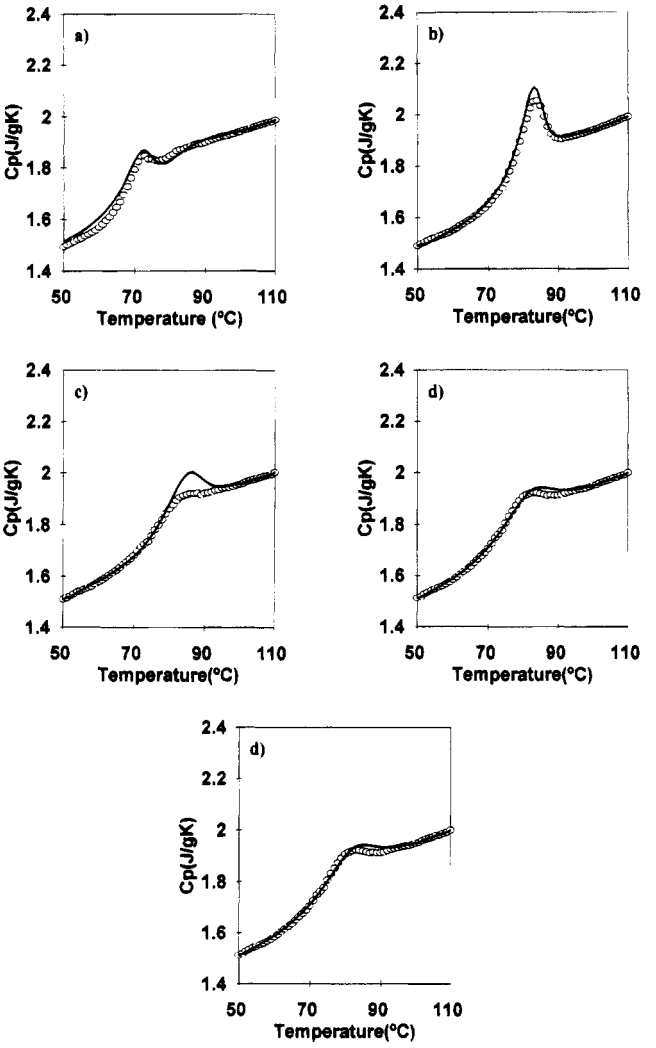

Figure 3. Experimental $c_p(T)$ curves measured on PEMA after thermal histories that include an isothermal annealing at 43 °C for 1000 min (a), 63 °C for 1000 min (b), and 73 °C for 2500 min (c) and after cooling at 1 °C/min (d) and 20 °C/min (e). The solid line represents the prediction of the model with Δc_p according to (6), B = 2000 J/g, and the remaining parameters as shown in Table 3. The circles correspond to the experimental values.

Table 1

	T_g (°C)	$A1$ [J/(gK)]	$A2$ [J/(gK²)]	$\Delta c_p(T_g)$ [J/(gK)]	$\Delta c_p(T_g - 30)$ [J/(gK)]	$T_g\Delta c_p(T_g)$ (J/g)
PMMA	107	0.898	−0.001 64	0.28	0.32	106.4
PEMA	70	0.747	−0.001 53	0.22	0.27	75.5
PBMA	37	0.703	−0.001 63	0.20	0.24	62

enough in the glassy state; in our work it is the temperature selected for the start of the measuring scans.

The values of $T_g = T_f$ for the three polymers are given in Table 1. The annealing temperatures were fixed as T_g − 27 °C, T_g − 7 °C, and T_g + 3 °C, the annealing times were around 1000 min in the two lowest temperatures and around 2000 min in the highest one. The fitting routine also employed the $c_p(T)$ curve measured after a cooling at 1 °C/min and the reference scan.

3. Results

The $c_p(T)$ curves measured for the three polymers after the five thermal treatments described in the experimental section (Figures 2−4) show several common features. A peak appears in the curve measured after cooling at 1 °C/min, but no peak appears in the reference scan. The isothermal treatment at the lowest annealing temperature, T_g − 27 °C, produces a peak within the glass transition interval in the $c_p(T)$ curve, whereas the isothermal annealing at T_g − 7 °C and T_g + 3 °C produces a peak which overlaps the high temperature side of the glass transition interval. The peak appearing after the annealing at the highest temperature is lower than the one corresponding to the annealing at T_g − 7 °C even if the annealing time is greater because at this temperature the initial state of the isothermal stage, reached after the cooling from T_0, is closer to equilibrium the higher the annealing temperature is. In fact, the $c_p(T)$ curve measured in PBMA after the annealing at T_g + 3 °C does not show a peak.

The differences between the results obtained in the different polymers lies mainly in the width of the temperature interval in which the glass transition takes place, which grows as the side-chain length of the polymer increases in the sequence PMMA−PEMA−PBMA. This fact is more apparent when the influence of the thermal treatment is analyzed in a plot of the difference between the $c_p(T)$ curve measured after a thermal treatment and the reference scan. Such a plot in some way separates the effect of the isothermal annealing from the effect of the cooling from equilibrium

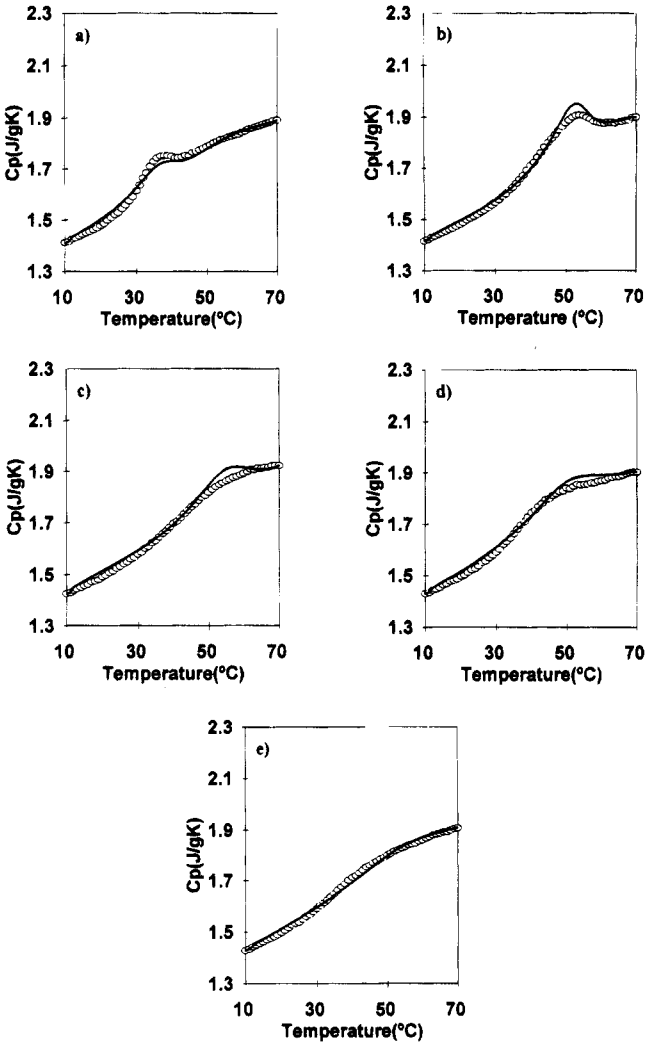

Figure 4. Experimental $c_p(T)$ curves measured on PBMA after thermal histories that include an isothermal annealing at 11 °C for 1000 min (a), 31 °C for 1000 min (b), and 41 °C for 2500 min (c) and after cooling at 1 °C/min (d) and 20 °C/min (c). The solid line represents the prediction of the model with Δc_p according to (6), B = 2000 J/g, and the remaining parameters as shown in Table 4. The circles correspond to the experimental values.

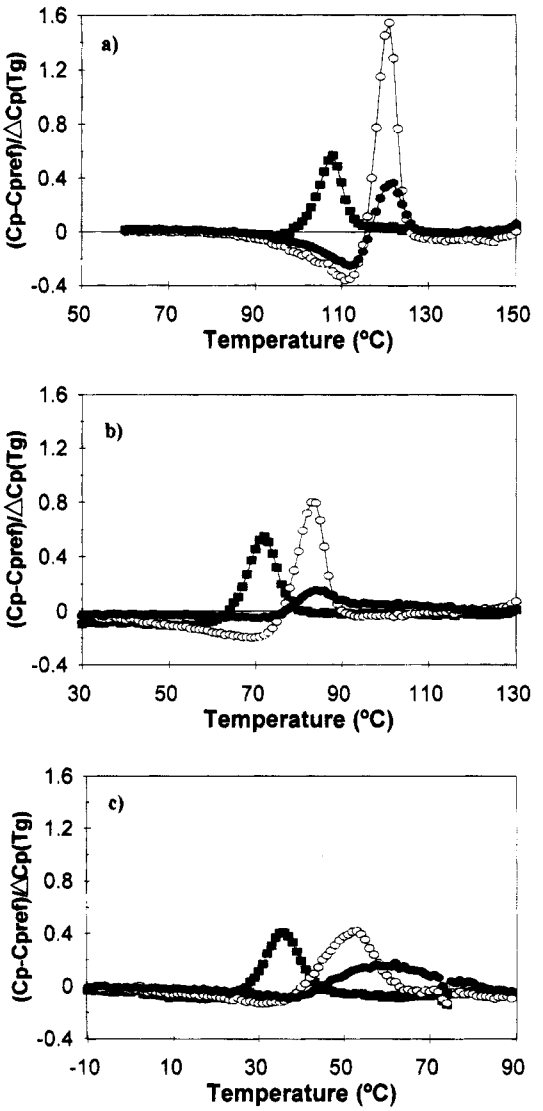

Figure 5. Difference between the $c_p(T)$ curve of the reference scan and the curves measured after an isothermal annealing at T_g − 27 °C (■), T_g − 7 °C (○), and T_g + 3 °C (●) (see text) for (a) PMMA, (b) PEMA, and (c) PBMA.

to the temperature of the start of the heating scan. Figure 5 shows these plots for the three polymers, normalized with the increment of heat capacity in T_g to enhance the comparison. The details of the calculation of $\Delta c_p(T_g)$ are given below. The characteristic shape of these plots[8,24,25] corresponding to $c_p(T)$ curves measured after isothermal annealings can be appreciated. The difference $c_p(T) - c_{p\,ref}(T)$ is negative in the low-temperature part of the glass transition and then becomes positive, showing the characteristic peak at a temperature which depends on the annealing time and annealing temperature. It is very clear that the peaks in these curves get significantly wider and lower as the side-chain length increases. The difference in the peak of the curve measured after the annealing at T_g − 27 °C in the three polymers is small than in the rest of the annealing treatments, but the effect is still present.

The dependence on temperature of the equilibrium heat capacity $c_{pl}(T)$ was determined by least-squares fitting the experimental values of $c_p(T)$ at temperatures higher than T_g + 20 °C to a straight line. In a similar way, the heat capacity corresponding to the glassy state, $c_{pg}(T)$, was determined by fitting the experimental results at temperatures below T_g − 30 °C to a straight line. A linear dependence of the specific configurational heat capacity with temperature, as in (6), is thus assumed. The values of $A1$ and $A2$ were determined for each polymer as averages of the values found in all the experimental scans and are shown in Table 1. The specific configurational heat capacity at T_g, also given in Table 1, decreases in the sequence PMMA–PEMA–PBMA, in good agreement with that found by other authors.[22,26] Nevertheless, our values are lower than those reported in these references, probably due to the fact that in the present work the straight line for $c_{pg}(T)$ is determined in a temperature interval quite close to the glass transition. Since, according to the data recommended in ref 22, the slope of the $c_{pg}(T)$ curve increases with temperature, the determination of $c_{pg}(T)$ from experimental values at lower temperatures would lead to smaller values of $c_{pg}(T)$ within the temperature interval of the glass transition.

4. Discussion

The modeling has been carried out by replacing the cooling and heating stages by a series of 1 deg temperature jumps followed by isothermal stages with a duration fixed to lead to the same overall rate of

Table 2. Model Parameters Found by the Search Routine in PMMA for Each Value of B and Each Expression for $\Delta c_p(T)$

B (J/g)	β	ln A (s)	T_2 (°C)	$T_g - T_2$ (°C)	D
		$\Delta c_p(T)$ as in Eq 6			
500	0.26	−26.9	64	43	4
1000	0.30	−39.6	48	59	8
2000	0.32	−53.3	23	84	16
3000	0.34	−60.7	3	104	24
4000	0.36	−66.4	−13	120	31
5000	0.38	−70.6	−27	134	40
		Δc_p Independent of Temperature			
2000	0.30	−45.8	6	101	22
		Δc_p as in Eq 7			
2000	0.32	−51.8	14	93	19

Table 3. Model Parameters Found by the Search Routine in PEMA for Each Value of B and Each Expression for $\Delta c_p(T)$

B (J/g)	β	ln A (s)	T_2(°C)	$T_g - T_2$ (°C)	D
		$\Delta c_p(T)$ as In Eq 6			
500	0.27	−29.5	22	48	6
1000	0.29	−40.4	2	68	11
2000	0.31	−52.6	−26	96	21
3000	0.33	−59.9	−46	116	32
4000	0.35	−63.5	−65	135	42
5000	0.35	−68.3	−78	148	53
		Δc_p Independent of Temperature			
2000	0.28	−45.6	−47	117	31
		Δc_p as in Eq 7			
2000	0.31	−52.5	−35	105	27

Table 4. Model Parameters Found by the Search Routine in PBMA for Each Value of B and Each Expression for $\Delta c_p(T)$

B (J/g)	β	ln A (s)	T_2 (°C)	$T_g - T_2$ (°C)	D
		$\Delta c_p(T)$ as in Eq 6			
500	0.25	−26.7	−18	55	7
1000	0.26	−35.3	−41	78	13
2000	0.28	−44.7	−72	109	25
3000	0.29	−49.8	−94	131	38
4000	0.30	−53.3	−112	149	51
5000	0.31	−56.8	−125	162	61
		Δc_p Independent of Temperature			
2000	0.26	−40.4	−98	135	42
		Δc_p as in Eq 7			
2000	0.29	−46.3	−82	119	32

temperature change as in the experiments. The configurational entropy was calculated in time instants t_k by means of (1), and the relaxation time at this instant is then calculated using (3). This value of the relaxation time is used to calculate the reduced time at the subsequent time instant t_{k+1}, according to (2). After each temperature jump the reduced time was evaluated at time instants $t_k = 0.001 \cdot 2^k$ s, with integer k.

The model contains four fitting parameters: β, A, T_2, and B. There is a clear correlation between these parameters,[15] as happens also in the models of Narayanaswamy–Moynihan[2,8,28,29] and Scherer–Hodge.[8,9,17,30] Thus, several, quite different, sets of four parameters lead to nearly identical model predictions of $c_p(T)$ curves for a given thermal history. A least-squares search routine that considers all the parameters as variable leads to nonsensical results. To solve this inconvenience, one of the parameters must be kept constant while the remaining three are being calculated. Such a fixed value of one of the parameters could perhaps be obtained from a different independent experimental technique or theoretical consideration. Or, simply, an arbitrary value can be assigned to it and its influence

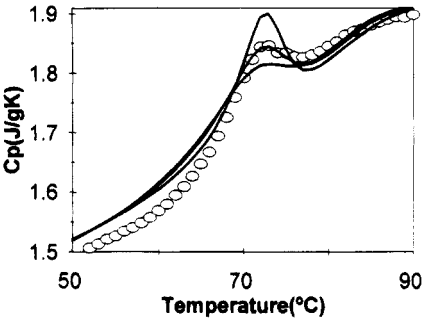

Figure 6. $c_p(T)$ measured on PEMA after a thermal history that includes an isothermal annealing at 43 °C for 1000 min. Model calculations with B = 500, 2000, and 4000 J/g (and the remaining parameters according to Table 2) are shown in solid lines. The peak appearing in c_p at approximately 72 °C decreases for increasing values of B; this identifies the different curves. The experimental results are represented as open circles.

on the value of the remaining parameters, determined by the search routine, can be studied. The last was the method followed in this work. The value of the parameter B was kept fixed, and β, T_2, and A were determined by a simultaneous least-squares fit to the five experimental $c_p(T)$ curves in Figure 2, 3, or 4, depending on the polymer under consideration. The Nedler and Mead[31] search routine was used. The simultaneous fit to the complete set of experimental results reflects the idea that the parameters must be material constants, independent of the thermal history and thus valid for all of them.

The set of three parameters determined in the search routine depends systematically on the value of B selected, as shown in Tables 2–4. The curves predicted by the model with any one of the sets of parameters shown in Tables 2–4 are very similar to those shown in Figures 2–4. The only exception is the $c_p(T)$ curve measured after an isothermal annealing at $T_g - 27$ °C. In this case, the curves predicted by the model with B less than 2000 J/g are higher than the experimental ones, as shown in Figure 6 for PEMA (the three polymers show exactly the same behavior).

The overall agreement between the experimental results and the theoretical predictions is quite good for the three polymers. It is noteworthy that the model predicts a peak in the $c_p(T)$ curve after an annealing at $T_g + 3$ °C always higher than the experimental, as found also in polycarbonate.[15] It has been impossible to fit simultaneously this curve and the ones measured after different thermal histories. This must be interpreted as a failure in some of the model's hypotheses. It does not seem likely that the problem lies in the assumed shape of the relaxation function, because this would affect any thermal history in a similar way. It could happen that the behavior of the relaxation times in states very close to equilibrium departs from the assumed form, since it is in the case of the isothermal annealing at temperatures within the high-temperature side of the glass transition interval where this anomaly is detected.

The parameter β that characterizes the shape of the relaxation function is quite independent of the value of B selected for the fitting procedure, but the parameters A and T_2 clearly correlate with B. When B increases, T_2 diminishes and the absolute value of ln A increases. Thus there are still different sets of four parameters that lead to model $c_p(T)$ curves which are very similar among themselves and very similar to the experimental

results. It seems that the only DSC experiments that can give information to choose the correct set of parameters are the heating scans measured after annealings at low temperatures. Still, in the case of the scans performed in this work, a very broad interval of B values would have to be accepted.

Although the value interval for B used in the calculations of this work is very broad, the results of different experimental techniques, mainly viscoelastic or dielectric experiments in the main relaxation region, can supply arguments to reduce significantly the uncertainty in the determination of this parameter (and, with it, that of the rest of the parameters of the model). As B increases, the difference $T_g - T_2$ also increases, attaining very unrealistic values; thus when $B = 3000$ J/g, $T_g - T_2$ is above 100 deg for the three polymers (see Tables 2–4), values higher than what is found by viscoelastic or dielectric techniques in these and other polymers.[19,32] Values of B below 1000 J/g give rise to peaks too high in the $c_p(T)$ curve measured after annealing at $T_g - 27$ °C. Even so, the uncertainty in the determination of B is still great. Other kinds of experimental techniques or theoretical arguments based on common characteristics of glass-forming materials (or of some specific class of them, as are polymers) are needed alongside DSC to reach a precise determination of the parameter values.

In spite of the uncertainty in the quantitative determination of the parameters B, T_2, and A, still the DSC results contain significant information on the material behavior of these polymers. Within the interval of B values between 1000 and 2000 J/g the β parameter can be determined to be 0.33 ± 0.02 for PMMA, 0.31 ± 0.02 for PEMA, and 0.27 ± 0.02 for PBMA. No such determinations are available for the KWW relaxation function from dynamic-mechanical or dielectric techniques. The difficulty here for their calculation lies in the vicinity of the main relaxation and the highest temperature secondary relaxation in these materials. Still, the dependence of the side-chain length of the parameter β is analogous to what is found for the main dielectric relaxation in poly(methyl acrylate), poly(ethyl acrylate), and poly(butyl acrylate).[33] It must be remarked that the uncertainty in the numerical values of the parameters B, T_2, and A does not entail an uncertainty in the curve of the relaxation times in equilibrium, $\tau^{eq}(T)$, determined by these three parameters,

$$\tau^{eq}(T) = A \exp\left(\frac{B}{TS_c^{eq}}\right) \tag{9}$$

with $S_c^{eq}(T)$ given by (5): as shown in Figure 7, the $\tau^{eq}(T)$ curves calculated with (9) for PEMA (the behavior in the other two polymers is exactly the same) with the different sets of parameters contained in Table 2 are practically coincident in the time interval relevant to the time scale of the measurements (the figure shows the time interval between 10^{-6} and 10^6 s). It can thus be stated that DSC determines uniquely the curve of equilibrium relaxation times *versus* temperature. Actually, the values of the relaxation times involved in the calculation of the reduced times are the ones corresponding to out-of-equilibrium states and not those of the $\tau^{eq}(T)$ curve, which represents a limit behavior. Nevertheless, since the model extends the validity of the Adam–Gibbs relationship to nonequilibrium states the behavior out of equilibrium is determined by the same parameters that define the equilibrium behavior. Thus, the fact that different sets of parameters B, T_2, and A define the same $\tau^{eq}(T)$ curve may explain why different sets of parametes determine the same $c_p(T)$ curve.

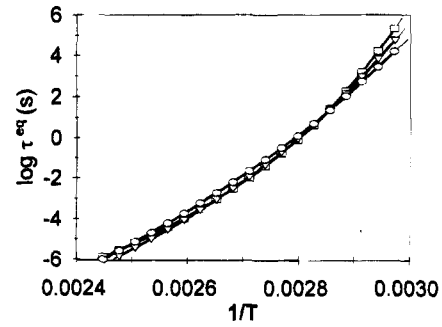

Figure 7. Equilibrium relaxation times (the value of the parameter τ in the KWW equation) calculated by the model for different values of B in PEMA (see text): (□) $B = 1000$ J/g, (▽) $B = 2000$ J/g, (○) $B = 4000$ J/g.

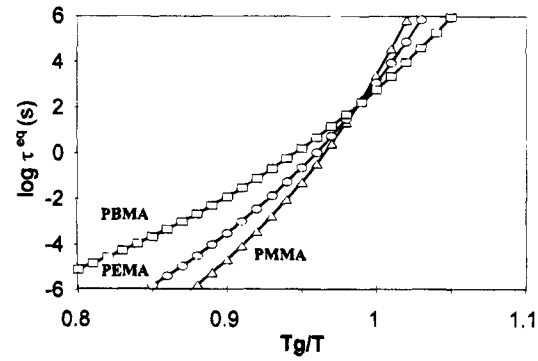

Figure 8. Equilibrium relaxation times calculated by (9) for the three polymers, with $B = 2000$ J/g and the remaining parameters according to Tables 2–4.

The $\tau^{eq}(T)$ curve, uniquely determined in this way from the DSC measurements, can itself be treated as a material function, instead of the quantities B, T_2, and A. As happens with the experimental $c_p(T)$ curves, this curve contains information on the behavior of the material not only at the temperatures at which the thermal treatment previous to the measuring was performed but also on the behavior at higher temperatures, the temperatures at which, in the measuring scan itself, the system approaches equilibrium. This is the temperature interval where the peak in the $c_p(T)$ curve appears, and it covers from 20 to 30 deg above T_g (Figure 1). The $\tau^{eq}(T)$ curves shift toward lower temperatures in the sequence PMMA–PEMA–PBMA, as T_g does. It is useful to compare these curves on a plot with T_g/T as abscissa, Figure 8. In order to simplify the diagram only the curves calculated with the set of parameters with $B = 2000$ J/g are shown. The curves cross each other at $T_g/T = 1$, as $\tau^{eq}(T_g)$ equals approximately 500 s in the three polymers. At temperatures above T_g the slope of the curve $\tau^{eq}(T_g/T)$ decreases as the side-chain length increases. The dependence of τ^{eq} on temperature for the three polymers can be compared with the help of the fragility parameter introdcued by Angell.[34] From the plot of Figure 8 it can be said that the behavior becomes "stronger" in the sequence PMMA–PEMA–PBMA. Numerically, the fragility parameter D is given by the equation

$$\tau^{eq} = A' \exp \frac{DT_2}{T - T_2} \qquad (10)$$

As D characterizes the curvature of the $\tau^{eq}(T)$ curves, it can be calculated from the parameters B, T_2, and ln A of our model. Thus, each set of parameters in Tables 2–4 determines a value for D, which was found by least-squares fitting. The value accepted for D was the one that minimized the difference between the $\tau^{eq}(T)$ curves calculated from (10) and from (9) with the parameter values from Tables 2–4. Because of the form of (9) and (10), the values of B and D are closely related. For a fixed value of B the fragility parameter D increases in the sequence PMMA–PEMA–PBMA.

The shape of the $\tau^{eq}(T)$ curves at temperatures above T_g can explain the widening of the peaks shown in Figure 5 as the side-chain length increases. A strong dependence of the relaxation times with temperature leads to a more rapid approach to equilibrium during the heating scan and in this way to narrower and higher peaks in $c_p(T)$. Of course this kind of argument has to be considered with care, since the approach to equilibrium depends on many factors, including the whole previous history (in fact, the values used in the calculation are not the equilibrium ones). Probably, the decrease of the value of the parameter β has an influence on the shape of the calculated $c_p(T)$ curves too.

The values of $\tau^{eq}(T)$ determined by DSC can be compared with the ones determined with viscoelastic or dielectric techniques. Figure 9 shows the τ_M *vs* T_g/T plot, $\tau_M(T)$ being the viscoelastic relaxation time obtained on the basis of the arbitrary assignment of a value of 100 s to the relaxation time in T_g and calculating the relaxation times at different temperatures from the shift factor $a_T(T) = \tau(T)/\tau(T_g)$ given in ref 32. The values of T_g in this calculation were the ones given in ref 32. Figure 10 shows the plot of the dielectric relaxation times τ_D *vs* T_g/T for the three polymers in this work obtained from ref 35. The relaxation times were calculated from isochronous curves of the imaginary part of the complex dielectric permittivity, ϵ'', in the main dielectric, or α, relaxation region. The reciprocal of the angular frequency of the measurement was taken as the relaxation time at the temperature of the maximum of the $\epsilon''(T)$ curve. Since no data for T_g are available for the samples used in ref 35, the T_g value used to draw the diagram of Figure 10 is the temperature of the maximum of the ϵ'' *vs* T curve measured at 0.01 Hz, with a procedure analogous to that employed for viscoelastic results. Differences between DSC, dynamic-mechanical, and dielectrical relaxation times have been reported for different glass-forming materials.[7,10,15] They are attributable to the different kind of motion in the relaxation process probed by each technique. Thus, dielectric "sees" the motion of the permanent dipole, which is located in our case in the lateral chain. The fact that dynamic-mechanical tests are relaxation processes whereas calorimetric and dielectric ones are retardation processes must also be taken into account when comparing the results of these techniques.[5] Finally, the procedure used to determine the mechanical and dielectric relaxation times was not exactly the same as that used for the calorimetric times, and this may have some influence on the results. This was due to the fact that for the polymers of this work the secondary β relaxation overlaps the main relaxation, and makes difficult an accurate determination of the parameters of the KWW equation from isothermal

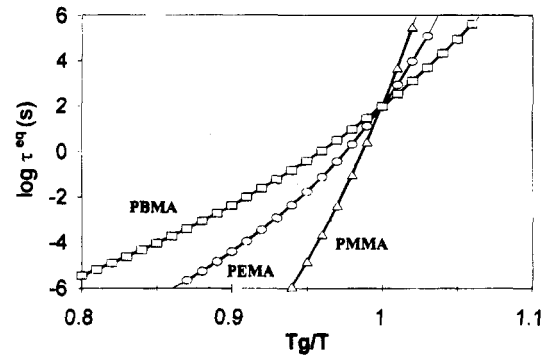

Figure 9. Viscoelastic relaxation times for PMMA, PEMA, and PBMA; see text.

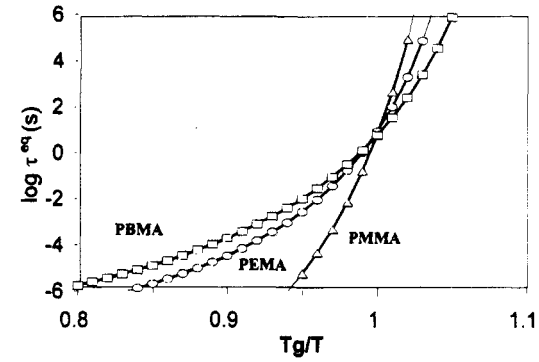

Figure 10. Dielectric relaxation times for PMMA, PEMA, and PBMA; see text.

dielectric or mechanical data. In our results the similarity of the behavior of the relaxation times determined by viscoelastic, dielectric, and calorimetric techniques is quite clear and supports the ability of the DSC technique, combined with a model for the structural relaxation, to determine important features of the behavior of materials in the vitrification process.

The determination of material parameters from DSC experimental results relies on a series of assumptions of the model: the KWW relaxation function and the expression for the dependence of the configurational heat capacity on temperature are two examples. It is interesting to analyze the influence of these choices on the material parameters obtained. In this work we focus on the last mentioned assumption.

As discussed in ref 15, there is not enough experimental evidence to adopt a specific expression for $\Delta c_p(T)$ and reject others. The equations of the model of the present work allow us to use different expressions for $\Delta c_p(T)$ and to compare the results of the fitting procedure. The calculations were conducted using (7), with the values of $T_g\Delta c_p(T_g)$ given in Table 1, and also by taking Δc_p as a constant independent of temperature. The value taken for Δc_p in this case was determined from (6), at the temperature $T_g - 30$ °C. This takes into account that at temperatures above $T_g - 30$ °C the heat capacity is slightly dependent on the thermal history (Figure 5) and thus has a certain configurational contribution. This value is also included in Table 1 for the three polymers. In Tables 2–4 the values of the parameters found by the search routine with $B = 2000$ J/g and the different expressions for $\Delta c_p(T)$ are shown. The influence of the expression for $\Delta c_p(T)$ on the $\tau^{eq}(T)$ curve is very small and is not shown. This lends additional support to the determination of the $\tau^{eq}(T)$ curve as a material function from the DSC results. The main influence of the $\Delta c_p(T)$ curve is on the values of

T_2 and A, because both parameters correspond to the limits of the $\tau^{eq}(T)$ curve at temperatures quite far from the experimental interval. Actually, the different curves selected for $\Delta c_p(T)$ for a given polymer are quite similar in the temperature interval from $T_g - 30$ °C to $T_g + 20$ °C but diverge significantly outside this interval.

5. Concluding Remarks

The model for the structural relaxation process here employed permits the determination of significant features of the material behavior in the temperature range of the glass transition from a limited set of experimental DSC results. A "calorimetric" $\tau^{eg}(T)$ curve and the form parameter β of the KWW relaxation function can be thus determined.

The slope of the $\tau^{eq}(T)$ curve at temperatures above T_g decreases in the sequence PMMA–PEMA–PBMA, in good agreement with data of the viscoelastic and dielectric main relaxation.

The β parameter of the KWW relaxation function decreases as the length of the side chain increases in the sequence PMMA–PEMA–PBMA.

Acknowledgment. This work was supported by the CICYT through the MAT 91-0578 project.

References and Notes

(1) Berens, A. R.; Hodge, I. M. *Macromolecules* **1982**, *15*, 756.
(2) Hodge, I. M.; Berens, A. R. *Macromolecules* **1982**, *15*, 762.
(3) Hodge, I. M.; Huvard, G. S. *Macromolecules* **1983**, *16*, 371.
(4) Berens, A. R.; Hodge, I. M. *Polym. Eng. Sci.* **1984**, *24*, 1123.
(5) Hodge, I. M. *J. Non-Cryst. Solids* **1994**, *169*, 211.
(6) Kovacs, A. J.; Aklonis, J. J.; Hutchinson, J. M.; Ramos, A. R. *J. Polym. Sci., Polym. Phys.* **1979**, *17*, 1097.
(7) Moynihan, C. T.; Macedo, P. B.; Montrose, C. J.; Gupta, P. K.; DeBolt, M. A.; Dill, J. F.; Dom, B. E.; Drake, P. W.; Easteal, A. J.; Elterman, P. B.; Moeller, R. P.; Sasabe, H. *Ann. N.Y. Acad. Sci.* **1976**, *279*, 15.
(8) Gómez Ribelles, J. L.; Ribes Greus, A.; Díaz Calleja, R. *Polymer* **1990**, *31*, 223.
(9) Romero Colomer, F.; Gómez Ribelles, J. L. *Polymer* **1989**, *30*, 849.
(10) Pérez, J.; Cavaille, J. Y.; Díaz Calleja, R.; Gómez Ribelles, J. L.; Monleón Pradas, M.; Ribes Greus, A. *Makromol. Chem.* **1991**, *192*, 2141.
(11) Más Estellés, J.; Gómez Ribelles, J. L.; Monleón Pradas, M. *Polymer* **1993**, *34*, 3837.
(12) Ruddy, M.; Hutchinson, J. M. *Polym. Commun.* **1988**, *29*, 132.
(13) Montserrat Ribas, S. *Prog. Colloid Polym. Sci.* **1992**, *87*, 78.
(14) Montserrat Ribas, S. *J. Polym. Sci., Polym. Phys.* **1994**, *32*, 509.
(15) Gómez Ribelles, J. L.; Monleón Pradas, M. *Macromolecules* **1995**, *28*.
(16) Scherer, G. W. *J. Am. Ceram. Soc.* **1984**, *67*, 504.
(17) Hodge, I. M. *Macromolecules* **1987**, *20*, 2897.
(18) Williams, G.; Watts, D. C. *Trans. Faraday Soc.* **1970**, *66*, 80.
(19) Adam, G.; Gibbs, J. H. *J. Chem. Phys.* **1965**, *43*, 139.
(20) Gibbs, J. H.; DiMarzio, E. A. *J. Chem. Phys.* **1958**, *28*, 373.
(21) DiMarzio, E. A.; Dowell, F. *J. Appl. Phys.* **1979**, *50*, 6061.
(22) Gaur, U.; Lau, S.; Wunderlich, B. B.; Wunderlich, B. *J. Phys. Chem. Ref. Data* **1982**, *11*, 1065.
(23) Moynihan, C. T.; Easteal, A. J.; DeBolt, M. A.; Tucker, J. *J. Am. Ceram. Soc.* **1976**, *59*, 12.
(24) Bauwens-Crowet, C.; Bauwens, J. C. *Polymer.* **1986**, *27*, 709.
(25) Cowie, J. M. G.; Ferguson, R. *Macromolecules* **1989**, *22*, 2307.
(26) Mathot, V. B. F. *Polymer* **1984**, *25*, 579.
(27) Narayanaswamy, O. S. *J. Am. Ceram. Soc.* **1971**, *54*, 491.
(28) Moynihan, C. T.; Crichton, S. N.; Opalka, S. M. *J. Non-Cryst. Solids* **1991**, *131–133*, 420.
(29) Tribone, J. J.; O'Reilly, J. M.; Greener, J. *Macromolecules* **1986**, *19*, 1732.
(30) Hodge, I. M. *J. Non-Cryst. Solids* **1991**, *131–133*, 435.
(31) Nedler, J. A.; Mead, R. *Comput. J.* **1965**, *7*, 308.
(32) Ferry, J. D. *Viscoelastic Properties of Polymers*; Wiley: New York, 1970.
(33) Gómez Ribelles, J. L.; Meseguer Dueñas, J. M.; Monleón Pradas, M. *J. Appl. Polym. Sci.* **1989**, *38*, 1145.
(34) Angell, C. A. *J. Non-Cryst. Solids* **1991**, *131–133*, 3.
(35) Gómez Ribelles, J. L.; Díaz Calleja, R. *Anal. Física* **1985**, *81*, 104.

MA9463324